Targeting PDE6D for inhibiting KRAS: A computational approach

1   Ayooluwa Ilesanmi[1#], Gbenga Dairo[2#*], Toheeb A. Balogun[3*], Bibiire Awoyale[4]

2   [1]Department of Chemistry, Mississippi University for Women, Columbus, U.S.A

3   [2]Department of Biological Sciences, Western Illinois University, Macomb, IL, U.S.A

4   [3]Department of Biological Sciences, University of California, San Diego, CA, U.S.A

5   [4]Department of Chemistry, University of Ilorin, Nigeria

6   [#]First author

7   *Correspondence: gs-dairo@wiu.edu (GD); tbalogun@ucsd.edu (TAB)

8

9   **ABSTRACT**

10   Lung cancer is the cancer of the lung's epithelial cells typically characterized by difficult breathing,

11   chest pain, blood-stained coughs, headache, and weight loss. If left unmanaged, lung cancer can

12   spread to other body parts. While several treatment methods exist for managing lung cancer,

13   exploring natural plant sources for developing therapeutics offers great potential in complementing

14   different treatment approaches. Several efforts have focused on inhibiting specific mutated genes,

15   including Epidermal Growth Factor Receptors and Anaplastic Lymphoma Kinase implicated in

16   lung cancer. In this study, we concentrated on inhibiting the mutated Kirsten rat sarcoma viral

17   oncogene homolog (KRAS) by targeting an associated protein (Phosphodiesterase 6δ) to which

18   KRAS form complexes. We evaluated bioactive compounds from Lingonberry (*Vaccinium vitis-*

19   *idaea* L), adopting computational approaches such as molecular docking, molecular dynamics

20   simulation, molecular mechanics/generalized Born surface area (MM/GBSA) calculations, and

21   pharmacokinetics analysis. A total of 26 out of 39 bioactive compounds of Vaccinium *vitis-idaea* L

22 had a higher binding affinity to the target receptor than the approved drug, Sotorasib. Further, the

23 pharmacokinetics properties of the lead compounds were examined, and the best four compounds,

24 namely, (+) – Catechin (Cianidanol), Arbutin, Resveratrol, and Sinapic acid, were further

25 subjected to molecular dynamic simulation. In conclusion, Arbutin (+) – Catechin and Sinapic acid

26 are predicted to be the best compound of *Vaccinium vitis-idaea* L. because of their

27 pharmacokinetic properties and drug-likeness attributes. Also, their stability to the target receptor

28 makes them a potential drug candidate that could be explored for treating KRAS-mutation-

29 associated lung cancer.

30
31
32
33 **INTRODUCTION**

34   Among all cancer types, lung cancer is prevalent and account for at least 18% of all cancer-

35 linked mortalities (Babar et al.). Cigarette smoking constitutes the major risk factor for the

36 development of lung cancer – with approximately 90% of lung cancer cases linked to cigarette

37 Ssmoking alone (Khuder). Consequently, smokers are prone to developing cancer cells and

38 resisting cancer treatment than non-smokers (Warren et al.). Essentially, lung cancer can be

39 classified into two main types namely, small cell lung cancer (SCLC) and non-small cell lung

40 cancer (NSCLC), with the latter accounting for approximately 85% of all lung cancer cases (Van

41 Meerbeeck et al.). There have been advances in studying oncogenes and mutation of tumor

42 suppressor genes toward the development of drug candidate for treating lung cancer (Herbst et al.;

43 Robichaux et al.; VanderLaan et al.; Yoda et al.). Among the targeted genes, a rat sarcoma viral

44 oncogene homolog, KRAS is implicated in many lung cancer cases (Shea et al.).

45   Rat sarcoma viral oncogene (RAS) has three isoforms namely, Human homologue of RAS,

46   Kirsten rat sarcoma viral oncogene, KRAS and the Neuroblastoma rat sarcoma viral oncogene,

47   NRAS (Barbacid; McBride et al.; Kirsten et al.; Chang et al.). Of the RAS isoforms, the KRAS

48   gene encodes two protein isoforms, KRAS-4B and KRAS-4A, with each consisting of 188 and

49   189 amino acids, respectively, due to different clipping of the fourth exon (Karnoub and

50   Weinberg). A wild-type KRAS has a glutamine amino acid at position 61 but, when the amino

51   acid at position 61 is substituted by histidine, it becomes a mutated KRAS. This mutation typically

52   occurs at codons 12 and 13. Significant efforts have concentrated on investigating KRAS

53   mutations especially for the discovery of specific inhibitors that could aid the treatment of KRAS

54   mutation lung cancer (McCarthy et al.; Kwan et al.). Until recently, KRAS had been widely dubbed

55   "undruggable" due to its lack of deep hydrophobic pockets, making it difficult to bind to small

56   molecules (Whaby et al.). However, the Food and Drug Administration (FDA) recently approved

57   a small molecule drug, Sotorasib, which specifically targets the RAS G12C mutation (Skoulidis et

58   al.). While the advances could help design more broad-spectrum therapeutics, the mutation

59   considered in the development of the drug is only found in low cases of lung cancer (∼13% of

60   lung adenocarcinoma) (AACR). Also, there have been reports of treatment resistance (Awad et

61   al.; Koga et al.). Hence, there is a need for continuous discovery of drug candidates for treating

62   KRAS mutation lung cancer.

63   Before the discovery of Sotorasib, efforts on directly targeting KRAS mutation have

64   historically achieved little success due to the complexity associated with KRAS mutations (Whaby

65   et al.). Since KRAS interacts with several proteins and are involved in many regulatory processes,

66   including cell growth and differentiation (Korzeniecki et al.), the inhibition of specific upstream

67   or downstream signaling pathways, membrane localization and protein interactions, can provide

68   an alternative pathway for discovering effective inhibitors for treating KRAS mutation lung

69   cancer. An important protein that KRAS interact with is phosphodiesterase 6δ (PDE6D) – termed

70   the trafficking chaperone of prenylated proteins (Yadav et al.). Phosphodiesterase 6δ (PDE6D) has

71   a beta-sandwich immunoglobulin fold which contains a hydrophobic pocket capable of binding to

72   the farnesyl group (Ismail et al.). Schmick et al. showed that PDE6D binds to and sequesters the

73   lipid of cytoplasmic RAS. Also, Zimmermann et al. showed that the manipulation of PDE6D

74   directly affects the localization and spatial organization of KRAS, which had implication on RAS

75   signaling. Since targeting KRAS directly might appear elusive, a focus on the KRAS: PDE6D

76   complex by targeting PDE6D can be an effective approach towards developing drug candidates

77   that could treat KRAS-mutation-associated lung cancer. Moreover, there have been reports on

78   indirect inhibitor discovery against PDE6D (Papke et al.; Zimmermann et al.).

79   Several plant or medicinal herbs have been identified and harnessed for treating diseases

80   due to their potent phytochemical constituents (Li et al.). In this study, we aimed at identifying

81   small molecule inhibitors present in Lingonberry (*Vaccinium vitis-idaea* L) against PDE6D which

82   is in complex with KRAS. Lingonberry (*Vaccinium vitis-idaea* L), found mostly across Central

83   Europe, Russia, and Canada, is a shrub identified as a good source of phenolic compounds with

84   promising therapeutic potentials (Gustavsson et al.; Kowalska et al.; Ștefănescu et al.). McDougall

85   et al. showed that extracts from berries including Lingonberry have antiproliferative effect on

86   cervical and colon cancer cells. Recently, Zhu et al. showed that Lingonberry extracts could inhibit

87   the proliferation of hepatoma cells (HepG2). Thus, we combined structural bioinformatics and

88   molecular modelling approaches in ligand-protein interaction analysis for developing potential

89   drug candidates for KRAS-mutation lung cancer.

90

91 **MATERIALS AND METHOD**

92 **Ligand and protein preparation**

93 The bioactive compounds assessed in this study were obtained from a study (Vilkickyte et al.)

94 which had evaluated phenolic compounds of Lingonberry (*Vaccinium vitis-idaea* L). The bioactive

95 compounds from the study, together with an FDA-approved drug (Sotorasib), were screened

96 virtually using the PyRx software (Python Prescription 0.8). The bioactive compounds and

97 Sotorasib 3D conformers in special data format (SDF) were retrieved from PubChem database,

98 while that of the protein (4JV8) was retrieved from Protein Data Bank (PDB). Polar hydrogen

99 atoms were added to refine the target protein using the Biovia Discovery Studio software

100 (v.21.1.0.20298) prior to docking.

101

102 **Molecular docking and molecular mechanics/generalized born surface area calculation**

103 First, the binding pocket scoring coordinates of PDE6D were determined by adopting the grid

104 generation module of Schrödinger Maestro 11.5. Next, the prepared ligands were docked into the

105 generated active site in the PyRx software (Python Prescription 0.8). The centers of the x, y, and z

106 generated grid were 26.1752, -12.4132, and -6.5578, respectively, while the dimensions

107 (Angstrom) of the x, y, z grid were 27.7133, 29.2607, and 12.6735, respectively. The advanced

108 quantum mechanics calculation was adopted via molecular mechanics generalized Born surface

109 area (MM/GBSA) to remove the false-positive values obtained from molecular docking. The

110 relative free energy for each PDE6D - ligand complex and the reference complex was computed

111 using the Maestro- Schrödinger suite under default parameters (Prime). The mathematical equation

112 adopted herein was as shown:

113 $$\Delta G\ bind = \Delta G\ complex - (\Delta G\ protein + \Delta G\ ligand)$$

114 **Pharmacokinetics Properties**

115 Following the virtual screening, the pharmacokinetic characteristics of the lead compounds with

116 the highest binding affinity were predicted for drugability, conformation to the Lipinski rule of

117 five conventions, and toxicity using the SwissADME web server (http://www.swissadme.ch/)

118 (Cheng et al.).

119

120 **Molecular dynamics and post-molecular dynamics simulation calculation**

121 To investigate the stability of the lead compounds to the target receptor, four compounds with the

122 highest binding affinity and promising pharmacokinetic properties were subjected to molecular

123 dynamics simulation for 100 nanoseconds (ns). The Schrödinger suite's Desmond program was

124 used to adopt energy-minimized receptor-ligand complexes, and the explicit solvent system was

125 employed to set up the molecular dynamics model (Shaw Research). The selected model was

126 created in a periodic box called a transferable intermolecular potential-4 point (TIP4P), which

127 permits a 10Å buffer region equidistance between protein atoms and box sides (Jorgensen et al.).

128 It was then upgraded with 0.15 M to reflect physiological conditions. At a temperature and pressure

129 of 300 K and 1.01325 bar, respectively, an appropriate quantity of counter sodium (Na+) and

130 chloride (Cl-) ions were utilized to neutralize the complete simulation model system. The entire

131 system was reduced by the minimization tool in the Desmond Maestro interface using the default

132 values of 1.0 kcal/mol, a 2000-iteration maximum, and a convergence threshold. Lastly, the

133 selected docked complexes were subjected to molecular simulation at 100 ns with default settings

134 using the OPLS-2005 force field (Schrodinger).

135   Furthermore, the simulation interaction diagram module of the Desmond program was used to

136   conduct more research on the root means square deviation (RMSD), root means square fluctuation

137   (RMSF), ligand torsion, and protein-ligand interactions profiling (Maestro). Thus, the trajectory's

138   root means square deviation (RMSD) was determined for each frame. The equation for RMSD for

139   frame x was as represented below:

140    $$\text{RMSDx} = \sqrt{\frac{1}{N} \sum\nolimits^{N} (i{=}1\ ri\ i\ (tx)) - ri\ (t_{\text{ref}})^2}$$

141   Where N denotes the number of atoms included in the atom selection; t_{ref} denotes the reference

142   time, and r' denotes the site of the atoms selected in frame x after superimposing on the reference

143   frame, where frame x is recorded at time tx. For every frame in the simulation trajectory, the

144   process is repeated. The equation for root means square fluctuation for atom I is represented below:

145    $$\text{RMSFi} = \sqrt{\frac{1}{T} \sum\nolimits < T\ t{=}1\ (ri\ i\ (t)) - ri(t_{\text{ref}}))^2 >}$$

146   Where T denotes the trajectory time over which the RMSF is calculated, tref denotes the reference

147   time; r denotes the site of atom i in the reference at time tref, and r' is the position of atom i at time

148   t after superposition on the reference frame.

149

RESULT AND DISCUSSION

151   **Molecular docking and molecular mechanics/generalized born surface (GBSA)**

152   Following the virtual screening of the thirty-nine bioactive compounds established from the

153   phenolic constituent of *Vaccinium vitis-idaea* L, twenty-five compounds showed higher binding

154   affinity in the active site of PDE6D when compared with the control, Sotorasib (Table 1). Further,

155   four compounds with high binding affinity and which conformed to the Lipinski rule of five

156   standard were identified (Table 2). From this study, Rutin had the highest binding affinity of -9.2

157   Kcal/mol; however, it was not considered for further analysis due to a violation of Lipinski rule of

158   five convention. Among the compounds which conformed to the Lipinski convention, (+) –

159   Catechin (Cianidanol), Arbutin, Resveratrol, and Sinapic acid were identified as potential drug

160   candidate because they can be considered druggable. Therefore, it can be inferred that they are the

161   best bioactive compounds of *Vaccinium vitis-idaea* L in the active site of PDE6D when compared

162   to the control Sotorasib (Table 1). Also, it can be inferred that the selected compounds can bind

163   better to PDE6D and interact with the amino residues, including, Ile129, Iles109, Arg61, Trp90,

164   Gln78 of the target receptor (Fig 4). To better ascertain the structural stability of the selected

165   compounds due to lack of accuracy in molecular docking, MMGBSA calculation was adopted to

166   determine the net receptor-ligand interaction. From this study, (+) – Catechin (Cianidanol) had the

167   highest value (-55.8 Kcal/mol) following MMGBSA calculation, which highlight its stronger

168   binding energy to 4JV8 compared to other compounds of Vaccinium vitis-idaea L (Table 2).

169

170   **Table 1:** Molecular docking result of the bioactive compounds in *Vaccinium vitis-idaea* L. and
171   control.

COMPOUND	CID[a]	BINDING AFFINITY (Kcal/mol)
Afzelin	5316673	-7.8
Arbutin	440936	-6.6
Vanillic acid	8468	-5.5
Syringic acid	10742	-5.1
Cryptochlorogenic acid	9798666	-8.4
Caffeic acid	689043	-6.3

Targeting PDE6D for inhibiting KRAS: A computational approach

Astragalin	5282102	-7.3
Avicularin	5490064	-7.7
Benzoic acid	243	-5.2
(+) – Catechin (Cianidanol)	9064	-8.1
Chlorogenic acid	1794427	-8.5
Cyanidin-3-arabinoside	12137509	-9
Cyanidin-3-O-galactoside	441699	-8.1
Cyanidin-3-O-glucoside	441667	-8
Ferulic acid	445858	-6.6
Hyperoside	5281643	-7.8
Isoquercitrin	5280804	-7.4
Kaempferol	5280863	-8.3
Nicotiflorin	5318767	-9
Neochlorogenic acid	5280633	-8.1
p-Coumaric acid	637542	-6.4
Procyanidin A1	9872976	-3.5
Procyanidin A2	124025	-2.9
Procyanidin B1	11250133	-1.1
Procyanidin B2	122738	-2.3
Procyanidin B3	146798	-2.4
Procyanidin C1	169853	
Protocatechuic acid	72	-5.5
Quercetin	5280343	-8.2

6"-O-acetylisoquercitrin	133554338	-8
Quercitrin	5280459	-8
Guaiaverin (Avicularin)	5490064	-7.7
Resveratrol	445154	-7.9
Reynoutrin	5320861	-9.5
Rutin	5280805	-9.2
Sinapic acid	637775	-6.5
trans-Cinnamic acid	444539	-6.1
Sotorasib	**137278711**	**-5.6**

172 [a]COMPOUND IDENTIFICATION NUMBER

173

174

175

176

177

178 **Table 2:** Molecular docking result of the compounds conforming to Lipinski rule of five with
179 binding affinity and MM/GBSA values

Compound	CID[a]	Binding Affinity (Kcal/mol)	MMGBSA (Kcal/mol)
(+) – Catechin (Cianidanol)	9064	-8.1	-55.8
Arbutin	440936	-6.6	-51.6
Resveratrol	445154	-7.9	-52.5
Sinapic acid	637775	-6.5	-42.4
Sotorasib	**137278711**	**-5.6**	**-46.2**

180 [a]COMPOUND IDENTIFICATION NUMBER

181

182 **Figure 1.** Post-molecular docking 3D profile of all simulated ligands with 4JV8

183
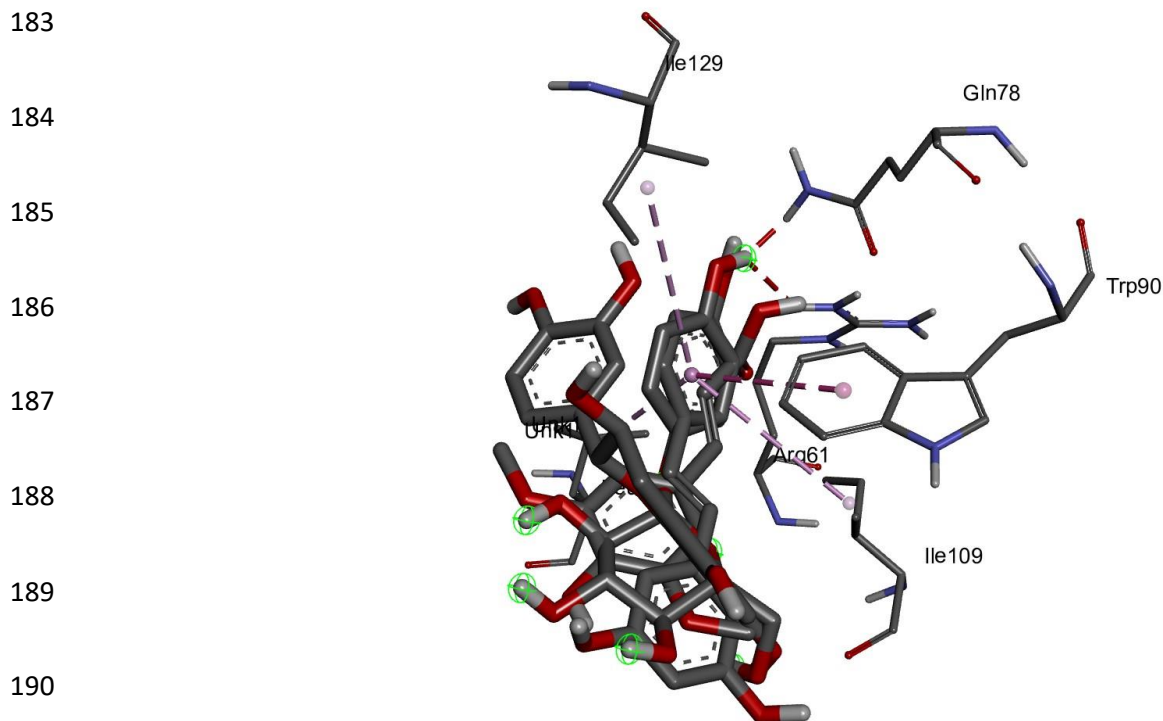
191

192 **Druggability Assessment**

193 The SwissADME web server (http://www.swissadme.ch/) was used to predict the drugability of

194 the selected compounds following the Lipinski rule of five. The rule states that a compound must

195 not violate > 2 rules to be considered druggable (Benet et al.). The rules include Molecular Weight

196 (MW) ≤ 500, Hydrogen Bond Donor (HBD) ≤ 5, Hydrogen Bond Acceptor (HBA) ≤ 10,

197 Lipophilicity (iLOGP) ≤ 5, and Molar Refractivity (MR) between 40 to 130 (Lipinski et al.). From

198 this study (Table 3), (+) – Catechin, Arbutin, Resveratrol, and Sinapic can be pursued as potential

199 drug candidates (Table 2).

200

201

202   **Table 3:** Drug-likeness prediction of plant Compounds

203

Compound	MW(g/mol)	HBD	HBA	iLOGP	MR	Lipinski Violation
(+) – Catechin (Cianidanol)	290.27	5	6	1.33	74.33	0
Arbutin	272.25	5	7	1.64	62.61	0
Resveratrol	228.24	3	3	1.71	67.88	0
Sinapic acid	224.21	2	5	1.63	58.12	0

204

205

206   **Molecular Dynamics and Post-Molecular Dynamics Calculation**

207   The selected bioactive compounds, which conformed to the Lipinski rule of five (Table 3), were

208   subjected to molecular dynamics (MD) simulation for 100 ns in the Desmond package (Figure 2).

209

210   **Figure 2.** The 2D structures of the selected bioactive compounds from *Vaccinium vitis-idaea* L.

211   and control: (A) (+) – Catechin (Cianidanol, (B) Arbutin, (c) Resveratrol, (D) Sinapic acid, (E)

212   Sotorasib.

213   A   B
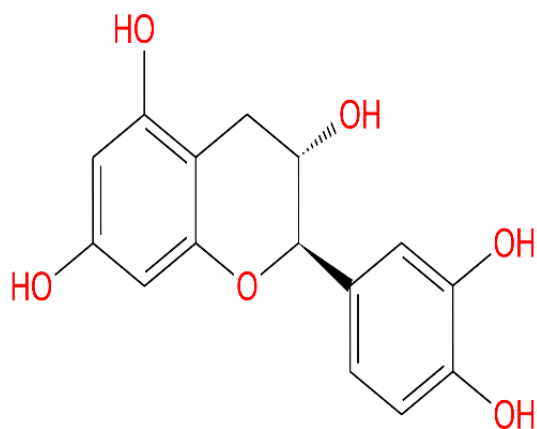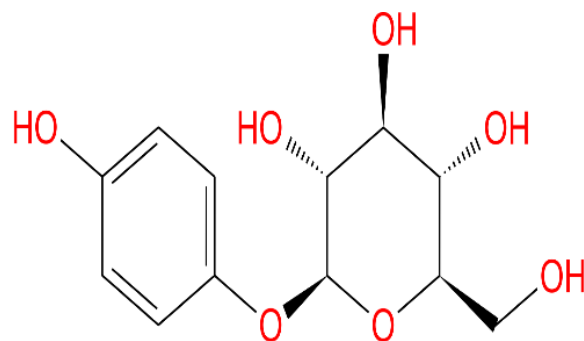
218

C

219   D

220

225

226

227

228

229   E

230

231

232

233

234

235
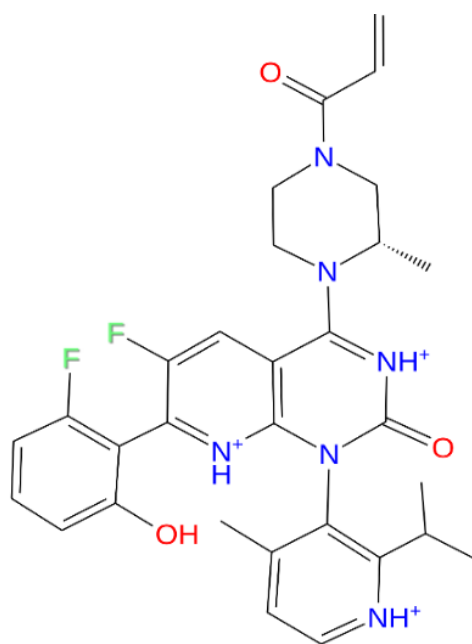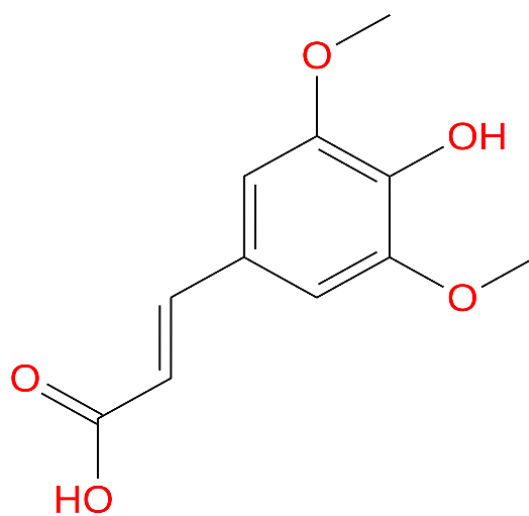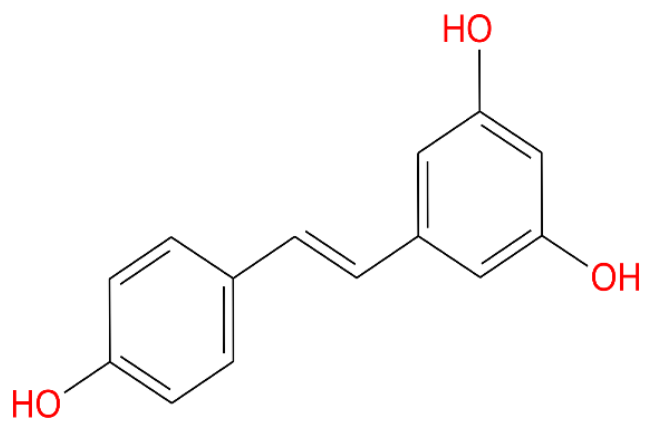
236   This analyzes the conformational stability, intermolecular interaction profiling, and binding site

237   occupancy of the compounds, which is critical in understanding the protein inhibition mechanism

238   based on docking data. During the simulation, the root means square deviation (RMSD), root mean

239   square fluctuation (RMSF), protein-ligand contacts, and protein/ ligand torsion were computed to

240   understand the conformational stability of the PDE6D ligand complex better. At the atomistic

241   level, this study showed an intermolecular contact formation between (+) – Catechin (Cianidanol),

242   Arbutin, Resveratrol, Sinapic acid, and the amino acid residues of PDE6D. The result suggests a

243   hydrogen bond interaction with TYR 149, ILE 109, CYS 56, GLN 78, ARG 61, ALA 112, GLU

244   110, SER 115, and GLN 116 during the simulation (Figure 3).

245

246   **Figure 3**. Structural view of ligand atom interactions with the protein residues: (A) (+) – Catechin

247   (Cianidanol, (B) Arbutin, (c) Resveratrol, (D) Sinapic acid

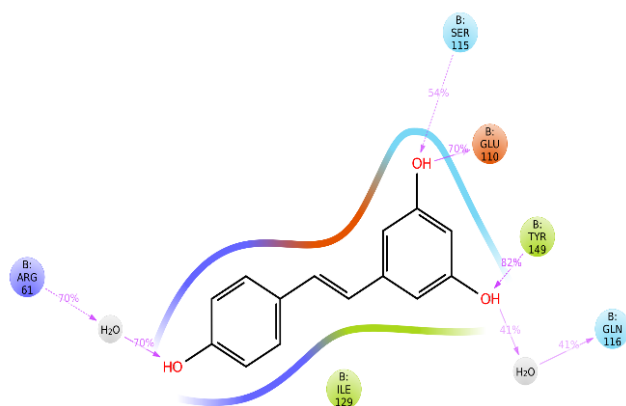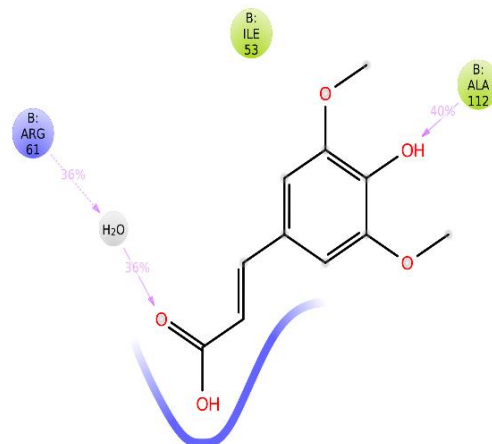248   A   B
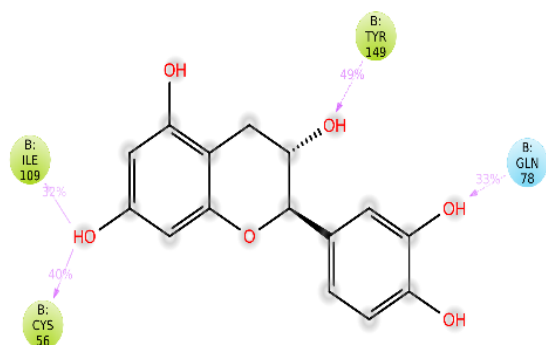
249

250
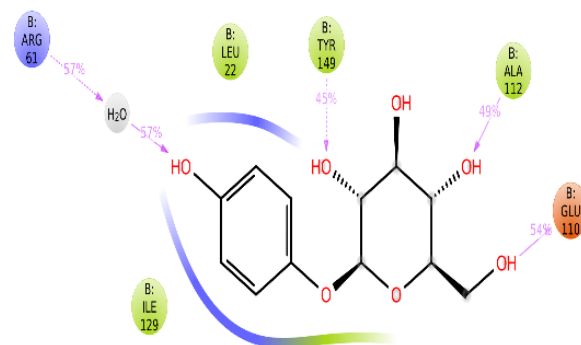
251   C

258

259

260   The Root Mean Square Deviation (RMSD) analysis helps to estimate how stable a compound is in

261   the binding pocket of a protein. In addition, it calculates the average change of displacement of the

262   protein-ligand complex during the simulation. In this study (Figure 4), the RMSD values for all

263   four ligands are stable and < 4 Å during the 100 ns simulation trajectories. (+) – Catechin

264   (Cianidanol) displayed a stable value of 0.4 Å to 1.6 Å at 0 ns to 75 ns, followed by a slight

265   elevation which became stable at 85 ns to 100 ns. Arbutin revealed stability from 0.45 Å to 2.8 Å

266   from 0 ns to 100 ns with a short-lived fluctuation to 3.3 Å. Resveratrol displays from 0.45 Å to 1.8

267   Å from 0 ns to 25 ns, fluctuated and became stable at 1Å to 1.65 Å from 25 ns to 100 ns. Sinapic

268   acid shows stability from 1.2 Å to 2.4 Å from 20 ns to 100 ns. Essentially, the four ligands showed

269   better RMSD values than Sotorasib, as they were more stable and had lesser fluctuations. The Cα

270   atoms in the PDE6D docked with the ligands in this study showed mean deviation <4 Å which is
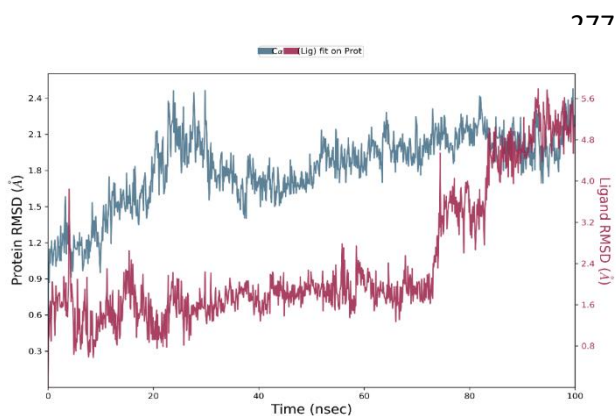
271   acceptable for small globular proteins.

272

273 **Figure 4.** Protein-Ligand RMSD of the compounds selected for molecular dynamics simulation.
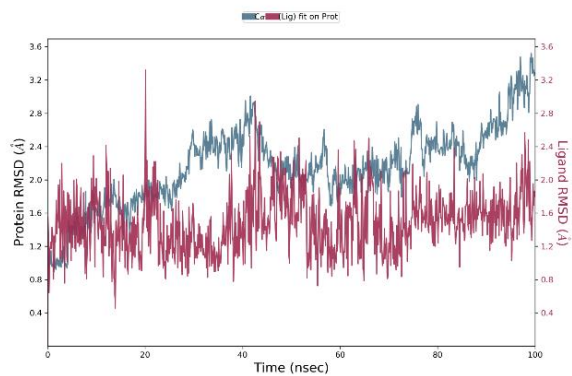
274 (A) (+) – Catechin (Cianidanol, (B) Arbutin, (C) Sinapic acid, (D) Sotorasib, (E) Resveratrol,
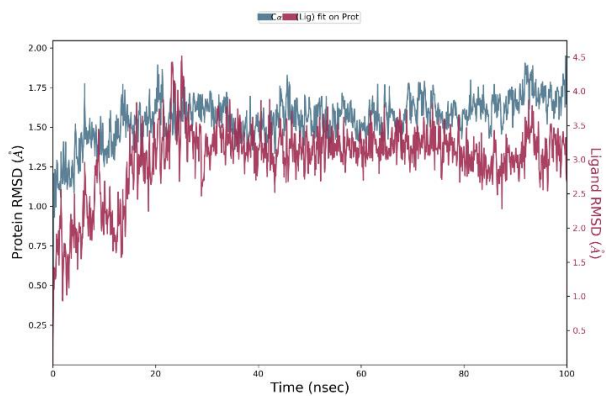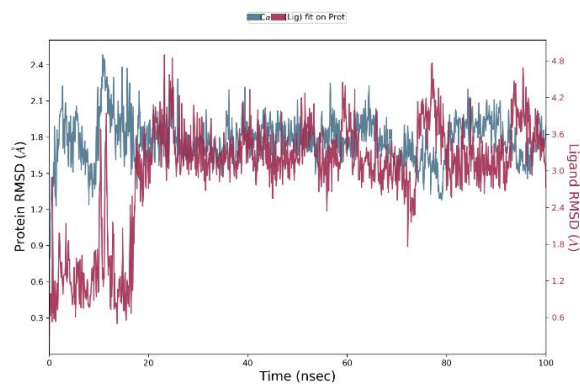
275

276 A   B
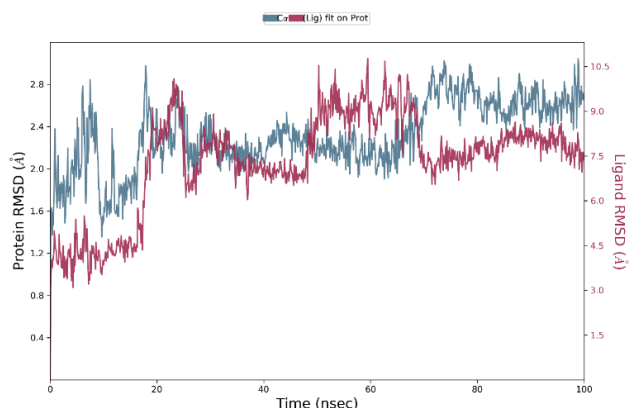
277

282

283

284 C   D

288   E

289

295   The structural changes that occurred per complex because of ligand binding were further

296   investigated. Thus, the root means square fluctuation (RMSF) was adopted to calculate the

297   residues' dynamic mobility structures following docking. According to the RMSF trajectory plot

298   (Figure 4), the protein amino acid residues of the docked complexes are moderately similar in their

299   fluctuation pattern during the simulation. However, Sotorasib (control) showed the highest

300   fluctuation with an RMSF value > 5.6 nm, suggesting that all the selected docked ligands are more

301   stable than the control in the active site of the target receptor. On this plot, peaks indicate areas of

302   the protein that fluctuate the most during the simulation. Particularly, the tails of protein chains

303   (i.e., N- and C-terminal) tend to fluctuate more while observing overall protein parts. In contrast,

304   the secondary structure elements, which includes alpha helices and beta strands, fluctuate less than

305   the loop regions because they are more rigid than the unstructured parts of the protein.

306

307

308 **Figure 5.** Protein-Ligand RMSF of the compounds selected for molecular dynamics simulation.
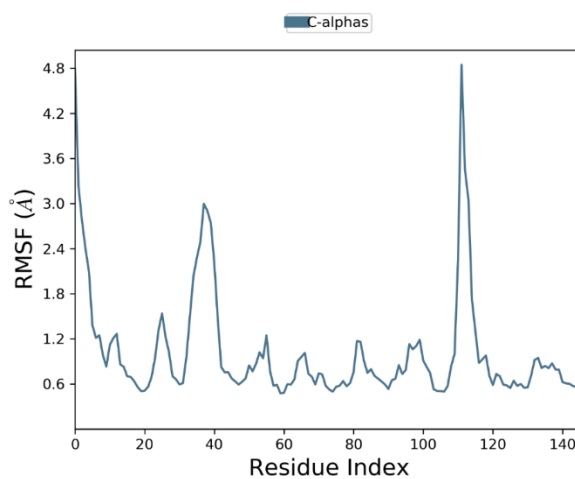
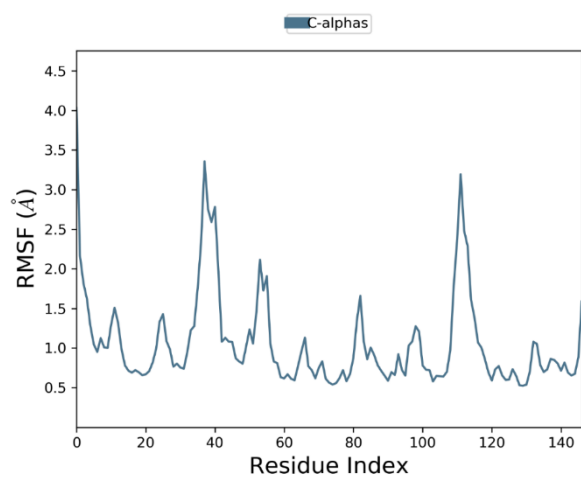309 (A) (+) – Catechin (Cianidanol, (B) Arbutin, (C) Resveratrol, (D) Sinapic acid, (E) Sotorasib
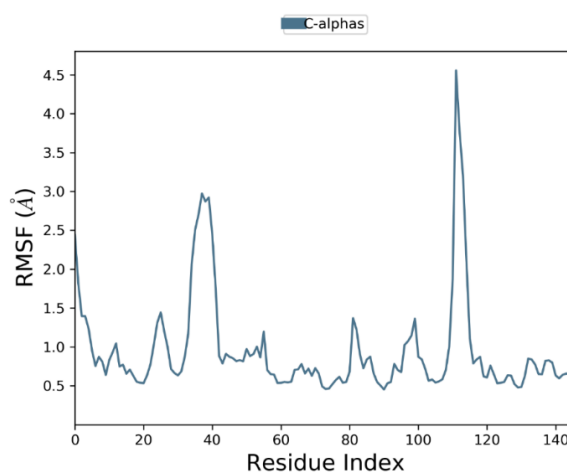
310

311   A   B
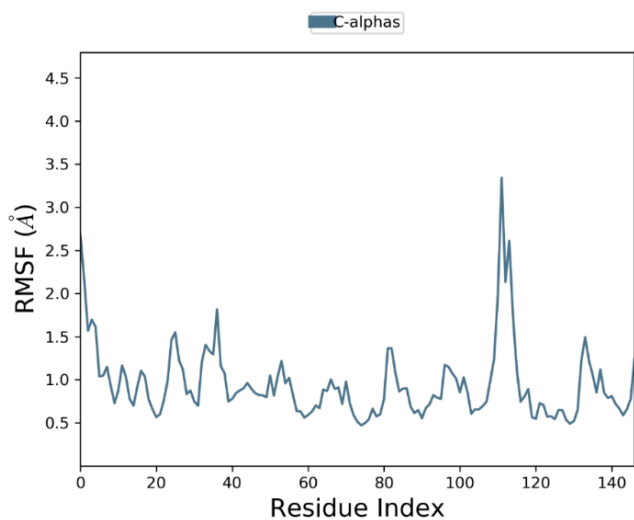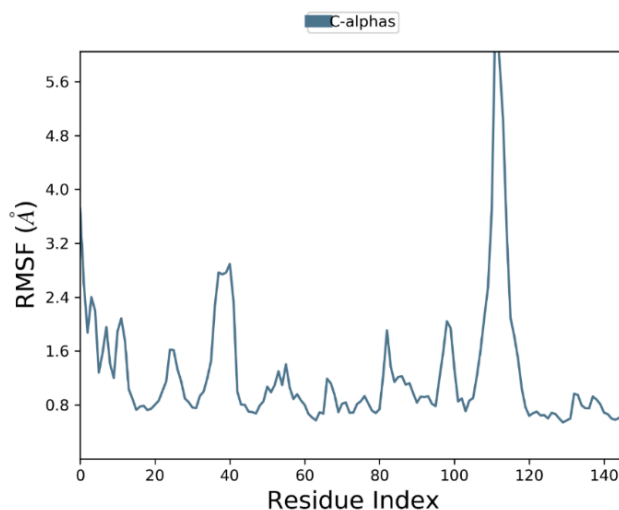

317

318

319   C   D

326
327
328
329
330
331
332

E

Protein-ligand interaction mapping

The stability of docked PDE6D-ligand complexes was investigated to determine intermolecular protein-ligand contacts, which are hydrogen bonds, ionic interactions, hydrophobic contacts, and water bridges (Figure 6). Interestingly, during the simulation, selected docked ligands exhibited good interactions with amino acid residues in the selective pocket of the PDE6D crystal structure. Furthermore, the selected docked compounds showed a higher hydrogen bond 0.8 than the control, which showed a hydrogen bond of 0.2. of arbutin has a value of 1.35. Hydrogen Bonds: (H-bonds) play a significant role in developing novel drug candidates because of their strong influence on drug specificity, metabolization and adsorption. Overall, it can be inferred from this study that compounds from Vaccinium vitis-idaea L. are relatively stable in the selective pocket of PDE6D compared to Sotorasib (control ligand).
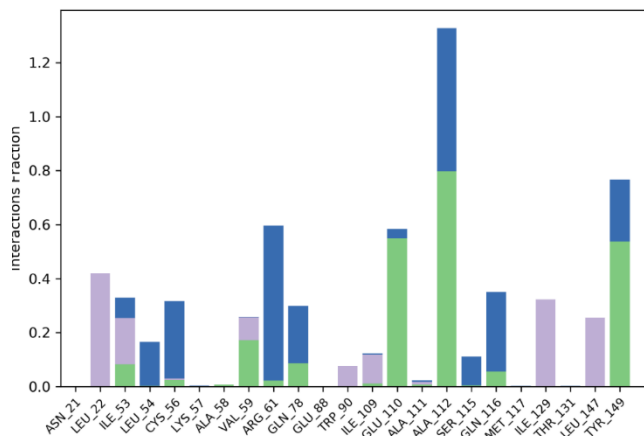
Figure 6. Stability of docked 4JV8-ligand complexes for hydrogen bonds, ionic interactions, hydrophobic contacts, and water bridges

346   A (+) – Catechin (Cianidanol)   (B) Arbutin

352

353
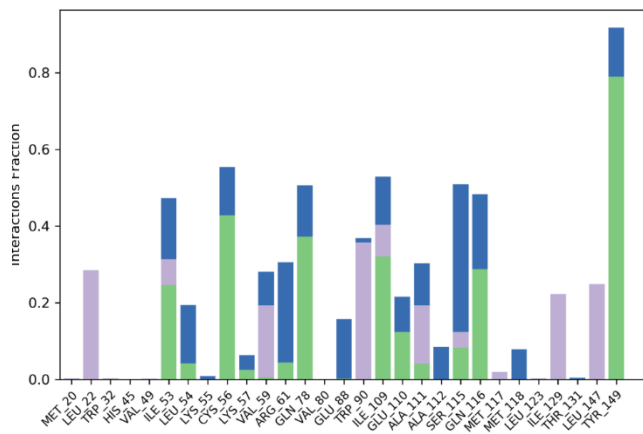
354   (C)Resveratrol   (D) Sinapic acid
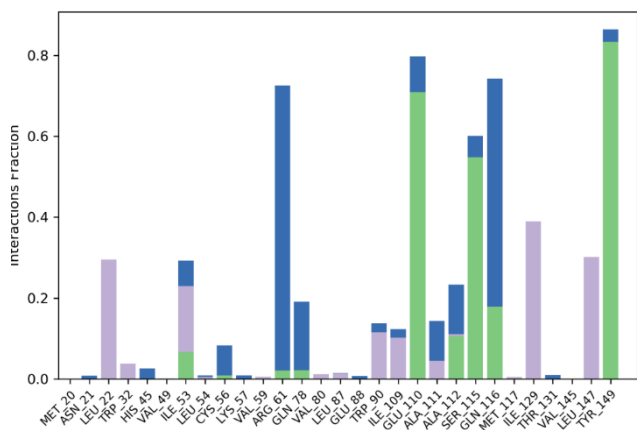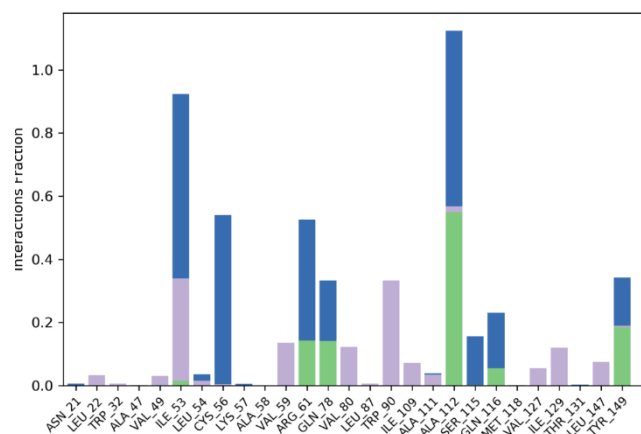
361

362

363

364   (E) Sotorasib

365

366

367

368

369
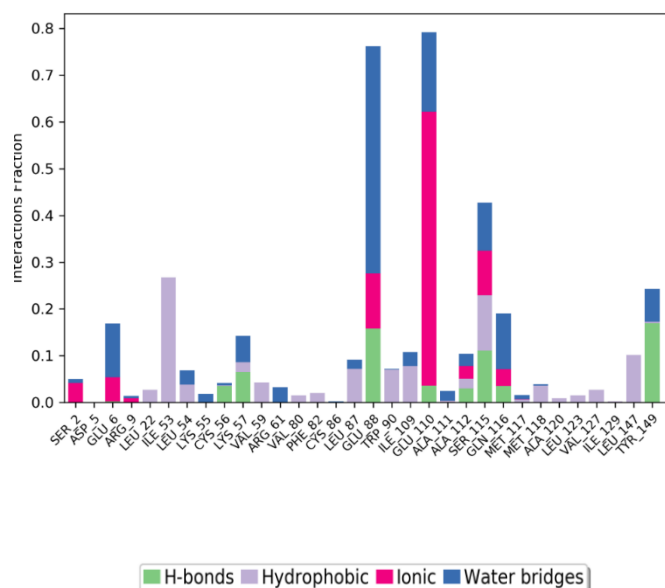
370

371

372   **Pharmacokinetics analysis and evaluation of ADMET properties**

373   In this study, the ADME properties of the selected compounds were examined to predict the

374   pharmacokinetic potentials of the bioactive molecules. The pharmacokinetic analysis (Table 4)

375   revealed that all the lead compounds of *Vaccinium vitis-idaea* L are easily absorbable. Also,

376   Arbutin, Resveratrol, and Sinapic acid are predicted to affect only the target receptor. Furthermore,

377   the ADME properties (Figure 5) showed that (+) – Catechin (Cianidanol), Arbutin, and Sinapic

378   could be recommended for further study because they do not cause a blood-brain barrier. Also,

379   they do not inhibit all the CYP 450 iso-enzymes, which is critical in drug metabolism.

380

381

382

383

384 **Table 4:** Pharmacokinetic Analysis of *Vaccinium vitis-idaea* L. Compound

S/N	Compound	TPSA (Å^2)	BA SCORE	PAINS
1	(+) – Catechin (Cianidanol)	110.38	0.55	1
2	Arbutin	119.61	0.55	0
3	Resveratrol	60.69	0.55	0
4	Sinapic acid	75.99	0.56	0

385
386
387
388
389
390
391
392
393
394
395

396 BA Score: Bioavailability Score.
397 TPSA: Topological polar surface area
398

399 **Table 5:** ADME predictions of *Vaccinium vitis-idaea* L. Compound

Property	(+) – Catechin	Arbutin	Resveratrol	Sinapic acid
Water Solubility	Soluble	Soluble	Soluble	Soluble
GI absorption	High	High	High	High
\Blood Brain Barrier permeant	-	-	+	-
P-glycoprotein substrate	+	-	-	-
CYP1A2 inhibitor	-	-	+	-
CYP2C19 inhibitor	-	-	-	-
CYP2C9 inhibitor	-	-	+	-
CYP2D6 inhibitor	-	-	-	-
CYP3A4 inhibitor	-	-	+	-

400

401   To inhibit KRAS, significant efforts have explored the KRAS-PDE6D complex. For example,

402   Zimmermann et al. showed that the reduction of plasma membrane localization of Ras through

403   PDE6D inhibition provides alternative opportunities for altering oncogenic Ras signaling.

404   Importantly, their result showed that a tested small molecule (Deltarasin) can alter the localization

405   of KRAS within the plasma membrane by transferring KRAS to the endomembrane. Their findings

406   revealed that the reported reduction in the proliferation of human pancreatic ductal

407   adenocarcinoma cell lines can be attributed to the Deltarasin-initiated relocation of oncogenic

408   KRAS. Consequently, the delocalization of RAS ultimately disrupts pathways activations and

409   provides a platform for inhibiting the activities of RAS (Canovas et al.). Using structure-based

410   ligand development, Papke et al. recently identified a novel inhibitor (Deltazinone 1) which was

411   shown to have anti-proliferative activity and exhibit lesser unspecific cytotoxicity than Deltarasin.

412   Thus, the discovery of these two inhibitors (Deltarasin and Deltazinone) has since opened new

413   frontiers on the exploration of complexes or interactions involving KRAS. In this study, we

414   successfully docked bioactive compounds against PDE6D which closely interacts with KRAS.

415   Among the selected best compounds, we identified Arbutin, (+)-catechin and Sinapic acid as

416   potential drug candidates. Arbutin has been considered as a candidate for treating many cancer

417   types. For example, Yang et al. showed that Arbutin can induce apoptosis in glioma cells which

418   confirmed its anticancer potency. Also, they established that Arbutin can significantly reduce the

419   associated-signaling proteins. Similarly, Safari et al. demonstrated the anti-cancer efficacies of

420   Arbutin for treating prostate cancer. Catechin or its derivative has been shown to have anti-cancer

421   potency. Di Leo et al. demonstrated that the application of a nanoformulation of (+)-catechin can

422   enhance the therapeutic efficacy of free (+)-catechin, which underscore the anti-cancer potential

423 of catechin. Similarly, findings from Sun et al. showed that catechin has inhibitory effect on lung

424 cancer cell proliferation.

425

426 **CONCLUSION**

427 Based on the findings from this study, it can be inferred that the best bioactive compounds

428 of *Vaccinium vitis-idaea* L. can be drugged against PDE6D of the KRAS: PDE6D complex in

429 human epithelial lung cancer cells. The binding affinity, MM/GBSA, protein-ligand interaction,

430 pharmacokinetics properties, and drug-likeness of the *Vaccinium vitis-idaea* L. compounds were

431 assessed compared to the FDA-approved drug (Sotorasib). After docking, 26 out of 39 bioactive

432 compounds had a higher binding affinity to the target receptor than Sotorasib. Following docking,

433 the 26 compounds were examined for drug-likeness, and the best four compounds, including {(+)

434 – Catechin (Cianidanol), Arbutin, Resveratrol, and Sinapic acid, were further processed to undergo

435 molecular simulation. The protein-ligand interaction after simulation showed that all four ligands

436 have good stability based on RMSD value < 4 Å which is within the acceptable threshold. Arbutin,

437 (+) – Catechin, and Sinapic acid is predicted to be the best compound of *Vaccinium vitis-idaea* L.

438 for treating lung cancer because of their pharmacokinetic properties and drug-likeness attributes.

439 Further *in vivo* and *in-vitro* analysis is required to establish the potency of the selected ligands in

440 this study for treating lung cancer associated with KRAS mutations.

441

442 **Author contributions**: GD and TAB designed the study. AI and BA performed virtual screening

443 and chemical library curation. GD, AI, and TAB performed molecular docking, pharmacokinetic

444 analysis, molecular dynamics simulation, and post-simulation analysis. AI wrote the first draft.

445 GD and TAB critically revised the manuscript. All authors read and approved the final manuscript.

446 **Informed consent statement**: Not applicable

447 **Data availability statement**: Not applicable

448 **Conflict of interest**: The authors declare no conflict of interest

449 **Acknowledgements**: We appreciate Dotun Olaoye for helpful input during the manuscript
450 preparation.

451

452 **REFERENCE**

453 AACR Project Genie Consortium, et al. "AACR Project GENIE: powering precision medicine
454 through an international consortium." Cancer discovery 7.8 (2017): 818-831.

455 Ahrendt, Steven A., et al. "Cigarette smoking is strongly associated with mutation of the K-ras
456 gene in patients with primary adenocarcinoma of the lung." *Cancer* 92.6 (2001): 1525-
457 1530.

458 Amato, Katharine A. Dobson, et al. "Tobacco cessation may improve lung cancer patient
459 survival." *Journal of Thoracic Oncology* 10.7 (2015): 1014-1019.

460 Awad, Mark M., et al. "Acquired resistance to KRASG12C inhibition in cancer." *New England*
461 *Journal of Medicine* 384.25 (2021): 2382-2393.

462 Babar, L., P. Modi, and F. Anjum. "Lung Cancer Screening. StatPearls. Treasure Island (FL)."
463 (2020).

464 Barbacid, Mariano. "Ras genes." Annual review of biochemistry 56.1 (1987): 779-827.

465 Bradley, Stephen H., Martyn Kennedy, and Richard D. Neal. "Recognising lung cancer in primary
466 care." *Advances in therapy* 36.1 (2019): 19-30.

467 Canovas Nunes, Sara, et al. "Validation of a small molecule inhibitor of PDE6D-RAS interaction
468 with favorable anti-leukemic effects." *Blood cancer journal* 12.4 (2022): 1-14.

469 Chang, Esther H., et al. "Human genome contains four genes homologous to transforming genes
470 of Harvey and Kirsten murine sarcoma viruses." Proceedings of the National Academy of
471 Sciences 79.16 (1982): 4848-4852.

472 Di Leo, Nicoletta, et al. "A catechin nanoformulation inhibits WM266 melanoma cell proliferation,
473 migration and associated neo-angiogenesis." European Journal of Pharmaceutics and
474 Biopharmaceutics 114 (2017): 1-10.

475 Gustavsson, Björn A. "Genetic variation in horticulturally important traits of fifteen wild
476 lingonberry Vaccinium vitis-idaea L. populations." *Euphytica* 120.2 (2001): 173-182.

477 Herbst, Roy S., Daniel Morgensztern, and Chris Boshoff. "The biology and management of non-
478 small cell lung cancer." *Nature* 553.7689 (2018): 446-454.

479 Ismail, Shehab A., et al. "Arl2-GTP and Arl3-GTP regulate a GDI-like transport system for
480 farnesylated cargo." *Nature chemical biology* 7.12 (2011): 942-949.

481 Karnoub, Antoine E., and Robert A. Weinberg. "Ras oncogenes: split personalities." Nature
482 reviews Molecular cell biology 9.7 (2008): 517-531.

483 Khuder, Sadik A. "Effect of cigarette smoking on major histological types of lung cancer: a meta-
484 analysis." *Lung cancer* 31.2-3 (2001): 139-148.

485 Kirsten, W. H., V. Schauf, and J. McCoy. "Properties of a Murine Sarcoma Virus1." Comparative
486   Leukemia Research 1969. Vol. 36. Karger Publishers, 1970. 246-249.

487 Koga, Takamasa, et al. "KRAS secondary mutations that confer acquired resistance to KRAS
488   G12C inhibitors, sotorasib and adagrasib, and overcoming strategies: insights from in vitro
489   experiments." *Journal of Thoracic Oncology* 16.8 (2021): 1321-1332.

490 Korzeniecki, Claudia, and Ronny Priefer. "Targeting KRAS mutant cancers by preventing
491   signaling transduction in the MAPK pathway." *European journal of medicinal*
492   *chemistry* 211 (2021): 113006.

493 Kowalska, Katarzyna. "Lingonberry (Vaccinium vitis-idaea L.) Fruit as a source of bioactive
494   compounds with health-promoting effects—A review." *International Journal of Molecular*
495   *Sciences* 22.10 (2021): 5126.

496 Kwan, Albert K., et al. "The path to the clinic: a comprehensive review on direct KRASG12C
497   inhibitors." *Journal of Experimental & Clinical Cancer Research* 41.1 (2022): 1-23.

498 Li, Fu-Shuang, and Jing-Ke Weng. "Demystifying traditional herbal medicine with modern
499   approach." *Nature plants* 3.8 (2017): 1-7.

500 McBride, O. W., et al. "Regional chromosomal localization of N-ras, K-ras-1, K-ras-2 and myb
501   oncogenes in human cells." Nucleic acids research 11.23 (1983): 8221-8236.

502 McCarthy, Michael J., et al. "Discovery of high-affinity noncovalent allosteric KRAS inhibitors
503   that disrupt effector binding." *ACS omega* 4.2 (2019): 2921-2930.

504 McDougall, Gordon J., et al. "Berry extracts exert different antiproliferative effects against
505   cervical and colon cancer cells grown in vitro." *Journal of agricultural and food*
506   *chemistry* 56.9 (2008): 3016-3023.

507 Papke, Björn, et al. "Identification of pyrazolopyridazinones as PDEδ inhibitors." *Nature*
508   *communications* 7.1 (2016): 1-9.

509 Robichaux, Jacqulyne P., et al. "Mechanisms and clinical activity of an EGFR and HER2 exon
510   20–selective kinase inhibitor in non–small cell lung cancer." *Nature medicine* 24.5 (2018):
511   638-646.

512 Safari, Hajar, et al. "Decrease of intracellular ROS by arbutin is associated with apoptosis
513   induction and downregulation of IL-1β and TNF-α in LNCaP; prostate cancer." Journal of
514   Food Biochemistry 44.9 (2020): e13360.

515 Schmick, Malte, et al. "KRas localizes to the plasma membrane by spatial cycles of solubilization,
516   trapping and vesicular transport." *Cell* 157.2 (2014): 459-471.

517 Shea, Meghan, Daniel B. Costa, and Deepa Rangachari. "Management of advanced non-small cell
518   lung cancers with known mutations or rearrangements: latest evidence and treatment
519   approaches." *Therapeutic advances in respiratory disease* 10.2 (2016): 113-129.

520 Skoulidis, Ferdinandos, et al. "Sotorasib for lung cancers with KRAS p. G12C mutation." *New*
521   *England Journal of Medicine* 384.25 (2021): 2371-2381.

522 Ștefănescu, Bianca-Eugenia, et al. "Chemical composition and biological activities of the nord-
523   west romanian wild bilberry (*Vaccinium myrtill*us L.) and lingonberry (*Vaccinium vitis-*
524   *idaea* L.) leaves." *Antioxidants* 9.6 (2020): 495.

525   Sun, Haiyan, et al. "Anti-cancer activity of catechin against A549 lung carcinoma cells by
526   induction of cyclin kinase inhibitor p21 and suppression of Cyclin E1 and P–AKT."
527   Applied Sciences 10.6 (2020): 2065.

528   Van Meerbeeck, Jan P., Dean A. Fennell, and Dirk KM De Ruysscher. "Small-cell lung
529   cancer." *The Lancet* 378.9804 (2011): 1741-1755.

530   VanderLaan, Paul A., et al. "Mutations in TP53, PIK3CA, PTEN and other genes in EGFR mutated
531   lung cancers: Correlation with clinical outcomes." *Lung cancer* 106 (2017): 17-21.

532   Warren, Graham W., Samantha Sobus, and Ellen R. Gritz. "The biological and clinical effects of
533   smoking by patients with cancer and strategies to implement evidence-based tobacco
534   cessation support." *The Lancet Oncology* 15.12 (2014): e568-e580.

535   Whaby, Michael, Imran Khan, and John P. O'Bryan. "Targeting the "undruggable" RAS with
536   biologics." *Advances in Cancer Research* 153 (2021): 237-266.

537   Yadav, Ravi P., and Nikolai O. Artemyev. "AIPL1: A specialized chaperone for the
538   phototransduction effector." *Cellular signalling* 40 (2017): 183-189.

539   Yang, Zhangkai, et al. "Arbutin exerts anticancer activity against rat C6 glioma cells by inducing
540   apoptosis and inhibiting the inflammatory markers and P13/Akt/mTOR cascade." Journal
541   of Biochemical and Molecular Toxicology 35.9 (2021): e22857.

542   Yoda, Satoshi, Ibiayi Dagogo-Jack, and Aaron N. Hata. "Targeting oncogenic drivers in lung
543   cancer: Recent progress, current challenges and future opportunities." *Pharmacology &*
544   *Therapeutics* 193 (2019): 20-30.

545   Zhu, Liangyu et al. "Inhibitory effect of lingonberry extract on HepG2 cell proliferation, apoptosis,

546   migration, and invasion." *PloS one* vol. 17,7 e0270677. 8 Jul. 2022,

547   doi:10.1371/journal.pone.0270677

548   Zimmermann, Gunther, et al. "Small molecule inhibition of the KRAS–PDEδ interaction impairs

549   oncogenic KRAS signalling." *Nature* 497.7451 (2013): 638-642.

550

551

552